



## A Mitral Heart Valve Prototype Using Sustainable Polyurethane Polymer: Fabricated by 3D Bioprinter, Tested by Molecular Dynamics Simulation

Z. S. Kazerouni<sup>1</sup>, M. Telloo<sup>2</sup>, A. Farazin<sup>1</sup>, S. Saber-Samandari<sup>3</sup>, E. Sheikhabaee<sup>4</sup>, B. Kamyab-Moghadasi<sup>5</sup>, H. Joneidi-Yekta<sup>3</sup>, S. Esmacili<sup>1</sup>, A. Khandan<sup>3,\*</sup>

<sup>1</sup> Department of Mechanical Engineering, Khomeinishahr Branch, Islamic Azad University, Isfahan, Iran

<sup>2</sup> Internal Medicine, School of Medicine, Firoozgar University Hospital, Iran University of Medical Sciences, Tehran, Iran

<sup>3</sup> New Technologies Research Center, Amirkabir University of Technology, Tehran, 15875-4413, Iran

<sup>4</sup> Student Research Committee, School of Medicine, Isfahan University of Medical Sciences, Isfahan, Iran

<sup>5</sup> Department of Chemical Engineering, Shiraz Branch, Islamic Azad University, Shiraz, Iran

**ABSTRACT:** Multiple diseases can cause deformities in the structure of the heart valve and the heart valve function, which leads to the patient's physical condition disorders and medical treatments like valve replacement surgery subsequently. In this case, artificial heart valves are used extensively, which generally are made of biocompatible (biologic) or metal (mechanical) materials. Thermoplastic Polyurethane is one of the best choices for the replacement of artificial heart valves due to their high mechanical stability, which makes the heart valve function last for a long-time. Therefore, the artificial heart valves were characterized by a scanning electron microscope analysis, and molecular dynamics simulation was conducted to predict the mechanical performance of the artificial heart valves in this study. Also, the tensile strength, strain at fracture, permeability, and the ultimate tensile strength were evaluated to monitor the mechanical property of these novel artificial heart valves. The obtained biological and mechanical properties of the vessel showed a suitable strain percentage at the fracture point and low permeability of the saline into the vessel. Also, about 11% increase in diameter, lead to a nearly 0.09 increase in mechanical performance. Although as surface analysis indicated, the permeability of the inner and outer layer of the artificial heart valves is in the range of 20% and 25%.

### Review History:

Received: 29/11/2019

Revised: 13/03/2020

Accepted: 03/05/2020

Available Online: 07/05/2020

### Keywords:

Heart Valve

Disease

3D Bioprinter

Polyurethane

Molecular

Dynamics Simulation

## 1. INTRODUCTION

One of the prevalent etiologies of heart disease is problem in the heart valves [1]. The heart has three tricuspid valves (pulmonary, aortic, and right atrioventricular or tricuspid) and one bicuspid (mitral). Tricuspid and mitral valves are located between the atrium and ventricles. These valves have four parts: leaflets, papillary muscles, chordae-tendinae, and annulus [2,3], which make the blood passing from the atrium to the ventricle while blocking their return to the atrium during the contraction phase of the ventricles, which is called systole. When the ventricles contract and the atrioventricular valves become closed, chordae-tendinae make the leaflets remain firmly in their place [4,5]. The other two valves are between ventricles and large arteries (aorta and pulmonary artery), which allow the blood to exit from the heart during the systolic phase and block the blood to return to the ventricles during the resting phase, the diastole. These two valves are semi-crescentic shape [6]. Pibarot et al. [6] designed a new heart valve with a selection of the optimal prosthesis and long-term management. They fabricate a novel Stented bio-prostheses purports to mimic the anatomy of the native aortic valve. Also, alternatives to warfarin therapy are now under investigation, including the use of direct

thrombin inhibitors administered at fixed doses. Myocardial infarctions can affect papillary muscles, and therefore, the valve becomes insufficient, and blood regurgitates to the atrium [7]. Aortic root dilation, enlargement of the ventricles, hypertension in the pulmonary artery, or aorta, make the aortic or pulmonary valves insufficient. Chronic rheumatic fever causes calcification in the valves and constricts the blood flow; thus, the valve becomes stenotic. Finally, a lot of valvular problems are congenital and diagnosed during childhood. Valvular problems, if left untreated, enlarge the heart and decrease the efficacy of its pumping [8–11]. Since the beginning of the heart valve replacement in the 1950s, several synthetic polymers, containing silicon material, have been used as valve leaflets. However, they could not be well-tolerated [10], therefore, from 1961 to 1963, researchers tested aortic heart valve based on polytetrafluoroethylene (PTFE), or Teflon, on 23 patients and had a high mortality rate as predicted. Studies then revealed that their leaflets were utterly stiff, thick, ruptured, and broken. Bio-stability is one of the essential features of the artificial heart valve, which is the ability of the material to tolerate destructing mechanisms. The degradation of polymers can be due to hydrolysis, oxidation, or even enzymatic catalysis, which accelerates the processes of hydrolysis, oxidation, lipid uptake, swelling, and

\*Corresponding author's email: amir\_salar\_khandan@yahoo.com



calcification [12]. Polymer stability is an essential factor in the body [13,14]. Long-term exposure to blood and then the accumulation of the calcium on valves' surfaces, known as the calcination phenomenon, prevent using those polymers in the implants [15]. Thermoplastic Polyurethanes (TPU) have been studied since the 1950s and are one of the most widely used materials in medical applications [16], due to their several desirable properties, including two-phase microstructure derived from hard crystalline segments and soft elastomeric segments. Other features, including blood compatibility and desirable hemodynamic behavior, are made polyurethane as an attractive material for cardiovascular applications. The use of polyurethane is extensive in cardiovascular applications today, which can be used in the manufacture of vascular catheters and stents, pacemaker cladding, and now artificial heart valves [17–25]. The use of polyurethane heart valves is critical in heart valve replacement surgery, but polyurethanes may cause calcification, which may cause valvular stiffness and disrupted structure. The calcification rate is affected by many phenomena such as local stress concentration, surface uptake of the plasma-bounded calcium molecules, the presence of any surface defects, and cell or mineral adhesions attached to the surface. The calcination level is dependent on the type of material and surface roughness, as well as the fluid flow shear rate [18]. Previous results showed that calcination of the polyurethane is a superficial phenomenon, which happens on the surface of the valve, and calcium cannot penetrate to the mid-substance. Three main hypotheses for calcination of polyurethane are factors related to the host individual, local stabilization conditions of the valve, and mechanical effects. Calcium sits effortlessly on stress-focused areas because lamination occurs mainly in areas with high mechanical changes, such as bending points of the Artificial Heart Valves (AHV's) leaflets [19]. Recently, Esmaeili et al. [25] fabricated novel artificial blood vessels using the fused deposition modeling (FDM) technique by evaluating their mechanical and biological properties. Del et al. [26] produced polycaprolactone (PCL) heart valve prosthesis using the electrospinning technique (ELS) with the evaluation of its in vitro functional characterization in a pulse duplicator. Also, the morphological investigation showed polymeric micrometric fibers randomly oriented with an average porosity of about 90%. This study was performed to produce and model an AHV using fused deposition modeling 3D bioprinter and applied using the molecular dynamics (MD) method to predict its mechanical and physical properties. The design new AHV for replacing with dysfunctional response HV using TPU and new bioprinter technique remarks this study as a novelty.

## 2. MATERIALS AND EXPERIMENTAL PROCEDURES

Fig. 1 (a-d) shows the heart value and heart mechanism in which the mitral valve dysfunction can be treated with sustainable polyurethane biopolymer valve manufactured by applying fused deposition modeling (FDM) and the mechanical properties were characterized by using a scanning electron

microscope (SEM) and molecular dynamic simulation process. In the first step, the AHV design was evaluated according to its natural structure and MRI images. The design file was converted to STL format and transferred to the appropriate software to simplify 3D for 3D printing, which optimizes 3D printing methods, as shown in Fig. 1 (a-b). Fig. 1 shows the designed model from the simplified 3D software: (a) lateral view, (b) top view. Also, the SEM image of the AHV surface fabricated using a 3D bioprinter technique with polyurethane polymer was shown to monitor the saline permeability in AHV. Fig. 2 (a-b) shows examining the different portions of the inlet valves, and the design was performed in Solid works software. Fig. 2 (a-b) shows a 10-chain polyurethane polymer simulation versus polymer simulation in a materials studio simulation box. According to the present studies in the field of 3D-printed heart valves, some studies evaluated different biocompatible materials for heart valves like silicon, polysiloxanes, and PTFE. Also, the purpose of this study is to investigate the kinetic energies and potential of a thermodynamic isolation system. At this stage, the system is subjected to 1 atmospheric pressure under NVE and the simulation time is considered 50 ps.

According to Fig. 3, the kinetic energy of the simulated polymer is 3500 kcal/mol, and the potential energy of the simulated polymer is 4000 kcal/mol. This software has advanced settings for printing, including 3D printer speed, nozzle head temperature, and the height of the layers. Proper settings for printing included the above as set out in the respective software. The 3D machine with nozzle head temperature, 220 °C, maximum forward speed: 180 mm/min, lower temperature to meet the initial layers at 70 °C, address layer thickness for 100 microns, percentage of material density for empty areas: 45%, layer Type: Bee House, the TPU was used and set for 3D bioprinter. To have negative slope angles to the upper levels of the valve inlet, the required segment needed to be supported, which was designed in the printer software. After the post-processing, the printout process was performed in the 3D simulation section of the software. After the final check and ensuring that the result was correct, the G-code file extracted from the printer software was transferred to the device. After loading the TPU filament with a diameter of 1.75 mm into the nozzle of the machine and after preheating it, the presence of appropriate fluidity was verified, and finally, the piece was ready to be printed. It took 4 hours for the heart valve to be printed, and the supports were separated from the final segment and prepared for subsequent tests and analyses. As can be seen, the printed heart valve is shown in Fig. 1(a-b) using fused deposition modeling tools and simplify 3D software by scanning the real heart valve in mimics software. In this study, the molecular dynamics method was used to extract the mechanical and physical properties of polyurethane polymer. The following steps have been taken to implement the molecular dynamics method: Simulation Box Preparation: At this point, the molecules of carbon, hydrogen, nitrogen, and oxygen are prepared, at random molecular ratios, are randomly placed in the simulation box. At this point, the atomic structure of the polyurethane molecule is formed ac-

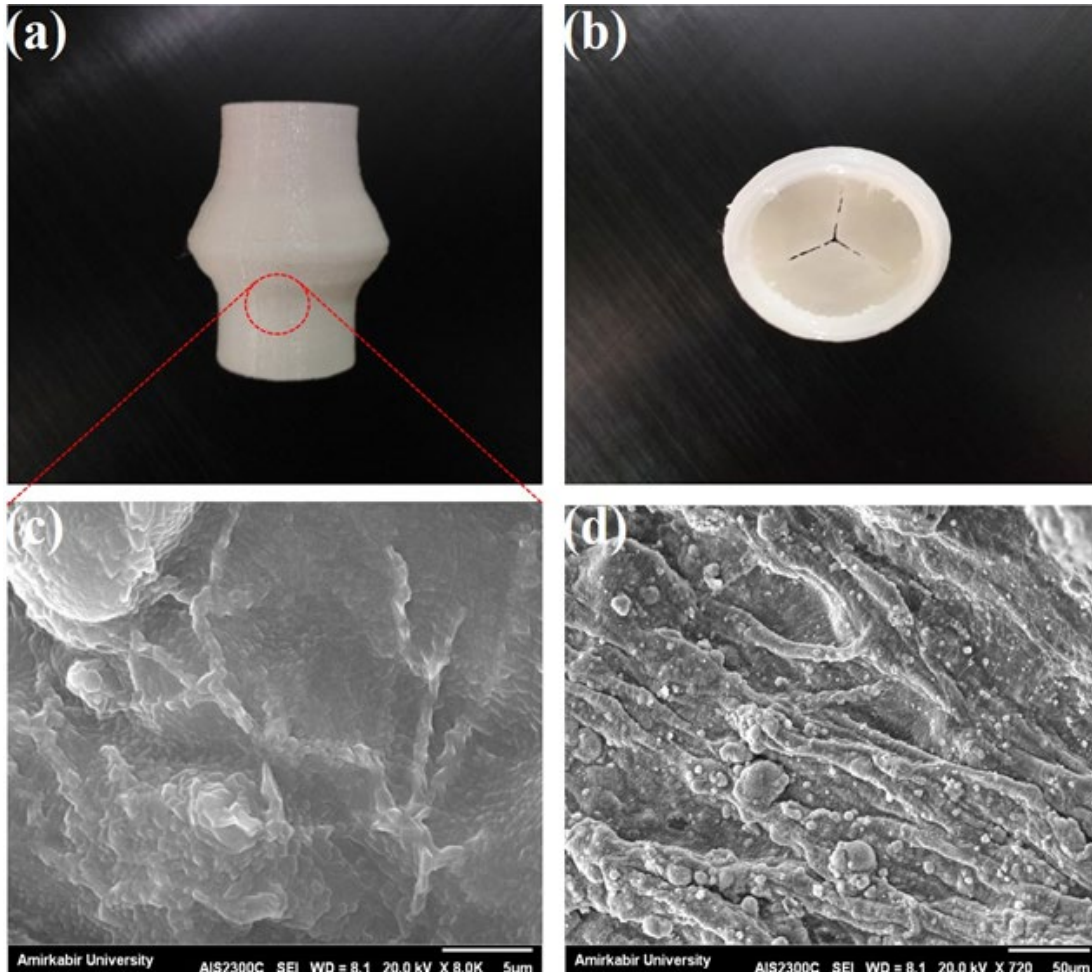


Fig. 1. Designed model transfer to the simplify 3D software (a) lateral view, (b) top view, SEM image (c) lateral view, (d) top view of AHV surface fabricated using 3D bioprinter technique with a polyurethane polymer

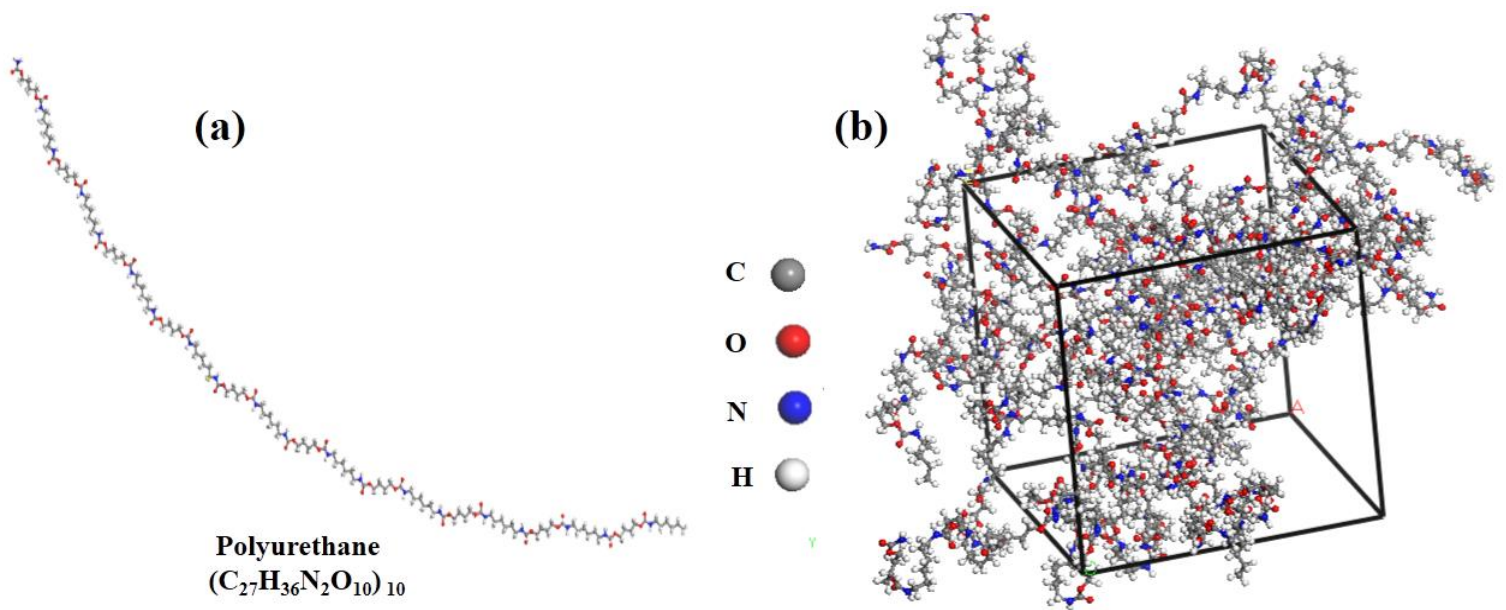


Fig. 2. The results of 10-chain (a) polyurethane polymer simulation, (b) Polymer simulation in the Materials studio simulation box

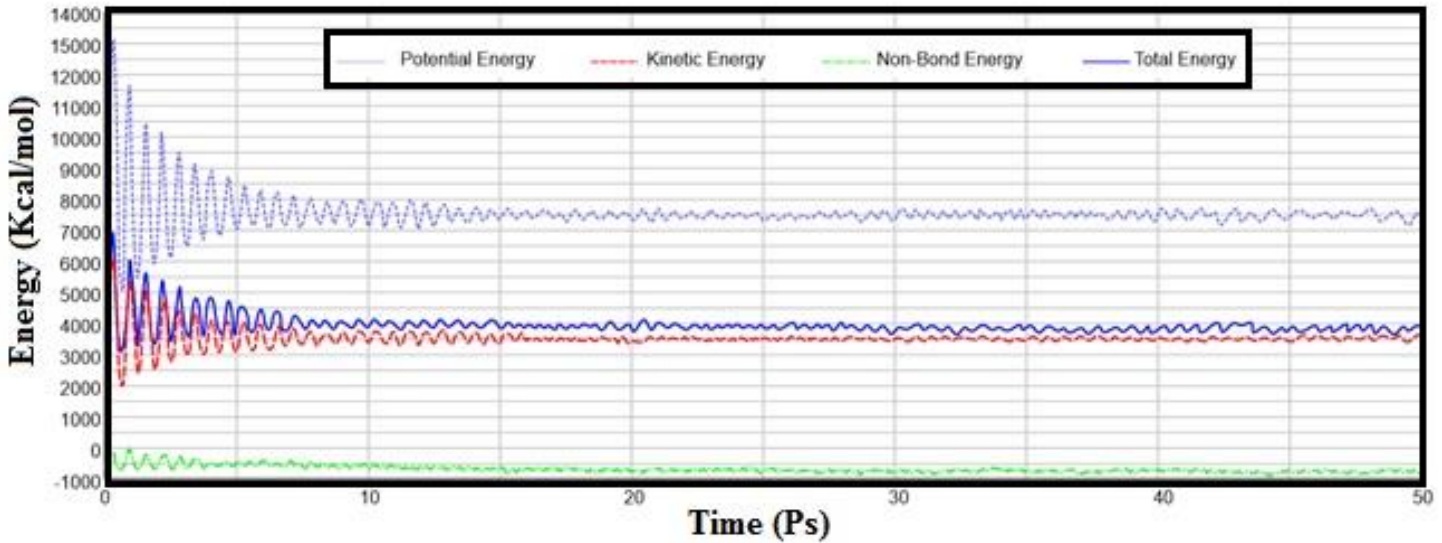


Fig. 3. Energy diagram of the polyurethane polymer in Materials Studio software

according to its chemical formula ( $C_{27}H_{36}N_2O_{10}$ ). The flexibility, permeability of the inner surface, and its biological property were evaluated in the simulated body fluid. The purpose of this study was to fabricate and model an AHV using fused deposition modeling 3D bioprinter and applied using the MD method to predict its mechanical properties (Young's modulus and Poisson's ratio) and physical properties (Density).

### 3. RESULT AND DISCUSSION

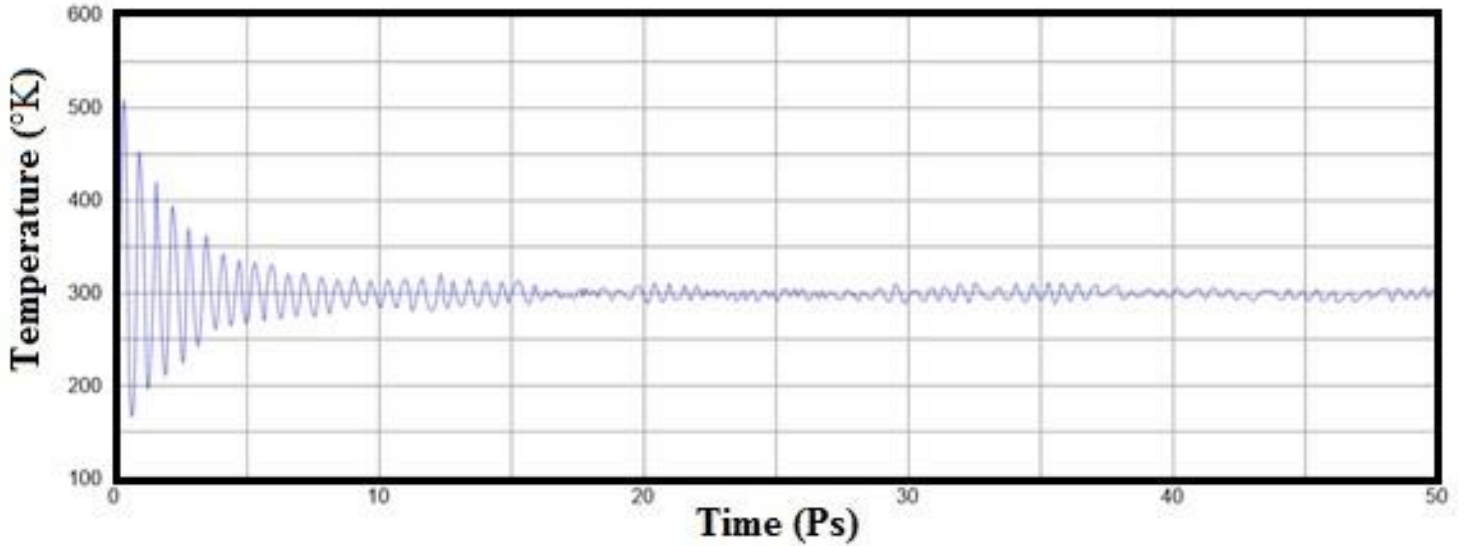
Heart valve replacement is one of the most challenging cardiac operations. This valve can be manufactured by biocompatible metals, use from animal (xenograft) or allogenic tissues, and nowadays, biotechnology-assisted materials, which make the polymeric valves. Mechanical heart valves are widely being used because of their longer life compared to tissue valves; however, hemolysis and blood coagulation are their problems, which makes the patients use life-long anticoagulant drugs, mostly warfarin. Polymeric valves are gaining attention due to their comparable durability and functioning time with mechanical valves and better hemodynamic function compared to tissue valves. Our knowledge of medicine is increasing exponentially. The prescriptions, as per pieces of evidence, evidence-based so-called drugs, are replacing the traditional medical practice by application of the same therapy for various patients. Finally, due to differences between human bodies from genetic changes to anatomical composition, individualized or personalized medicine has been evolved and developing very fast. The architecture of the human heart is very delicate and is working in good order. Heart valves are one of the most critical structures in the heart. They have two layers of endothelium and an arranged matrix bed of collagen and elastin fibers, which make this valve flexible, soft, elastic, and firm simultaneously. They have to confront three forces;

opening pressure from behind (shear stress), the reverse force which closes the valve from the front to avoid leaking the blood backward (tensile stress), and flexural stress which is induced transvascular when the valve is either open or closed. When the valve becomes stenotic due to calcifications, the opening pressure increases, and therefore, the chamber behind becomes hypertrophic (e.g., in aortic stenosis, the left ventricle has to become hypertrophic, and in mitral stenosis, the left atrium is hypertrophic). When the valve becomes insufficient, the blood regurgitates backward and makes the pumping process less efficient, and enlarges the affected chamber. Heart valve replacement for stenotic or insufficient valves makes the heart work better again. These artificial valves should fit the anatomy and the exact structures of the heart to achieve a better result; therefore, to adapt to personalized medicine, using 3D printing by computed tomography scans or magnetic resonance images can be very helpful. According to FDA approval protocols, the fabricated heart valves should have some baseline eligibility criteria in their functions (e.g., regurgitated volume, standard geometrical, and effective orifice area) to pass the first phase of the experiment and pharmacokinetics for a better quality of medical consultations [27–35] Although present studies have suggested impressive results about 3D-printed heart valves with biocompatible polymeric materials, they will become inefficient due to thrombosis formation, calcification, and multiple cyclic loading. One of the well-known and highly applicable biomaterials is polyurethane, which has been used for other purposes. In this research, we aimed to investigate the usage and applicability of polyurethane in the field of 3D-printed heart valves.

The MDs are one of the most precise techniques for real simulation in physics, which is used to simulate complex multi-particle systems. In this method, phase paths of systems

**Table 1. Physical and mechanical properties of the polyurethane polymer**

Physical and mechanical properties	Molecular dynamics simulation	Laboratory Mode
Density (g/cm <sup>3</sup> )	1	1.02 [12-13]
Young's modulus (MPa)	70	33-72 [12-13]
Poisson's ratio (–)	0.3	0.3 [12-13]

**Fig. 4. NVT at 300 K in the Materials Studio software**

involving thousands of interacting particles are obtained by solving Hamiltonian equations under appropriate and controlled conditions [36–45]. Analyzing the particle path in the phase space and applying statistical mechanics, which is a mediator between the microscopic and macroscopic quantities, information can be obtained on various properties of the system, including energy, structural, dynamic, mechanical properties. In MDs, the system's sequential configuration is obtained by integrating Newton's laws of motion. The result is a curve that shows how the positions and velocities of the system particles change over time. Using MDs paths, time-dependent thermodynamic properties can be calculated.

### 3.1. Molecular Dynamics Simulation Of The Polyurethane Polymer

For MDs, it is necessary to apply this term to the system after choosing the particles and the simulation space to apply the equation from the beginning of the simulation until the system reaches equilibrium in solving equations. Each of these modules determines a particular path to equilibrium during the simulation time. Choosing different artifacts in MDs can lead to different answers. NVE (constant number ( $N$ ), volume ( $V$ ), and energy ( $E$ ); the sum of kinetic ( $KE$ ) and potential energy ( $PE$ ) is conserved,  $T$  and  $P$  are unregulated) or Micro-focal (particle number and energy are constant) and the NVT or focal point (number of pressure and temperature

particles are constant). Isothermal-pressure NPT (number of pressure particles and temperature constant). At this stage, the simulation box is subjected to NVE at 300 K, while the simulation box, as shown in Fig. 3, is subjected to NVT loading at 300 K. This hybrid is performed to increase the system energy so that the atoms gain enough energy to move to the equilibrium. Fig. 3 illustrated the energy diagram of the polyurethane polymer in the Materials Studio Software. The reason for applying NVT was to release the molecular structure from the initial internal stresses that were applied when constructing the simulation box. At this stage, the initial system density (0.9 gr/cm<sup>3</sup>) is assumed to allow the molecules and atoms to move to the optimum state. The simulation time was 50 ps. At this stage, the system is subjected to 1 atm pressure and at 300 °C under NPT to obtain the density of the system closer to the actual density. Also, NPT can eliminate residual stresses of the system. The simulation time is 50 ps. According to Fig. 4, the first 10 polyurethane polymer chains were simulated in the Materials Studio Software. The output was used to derive mechanical properties (Young's modulus and Poisson's Ratio) and physical properties (density) using the universal force field. It should be noted that in this polymer is used 2700 carbon atoms, 3600 hydrogen atoms, 200 nitrogen atoms, and 1000 oxygen atoms, and its structure is cubic with dimensions 35 × 35 × 35 angstroms (Å<sup>o</sup>). At this stage, the box is subjected to an energy minimization process to accom-

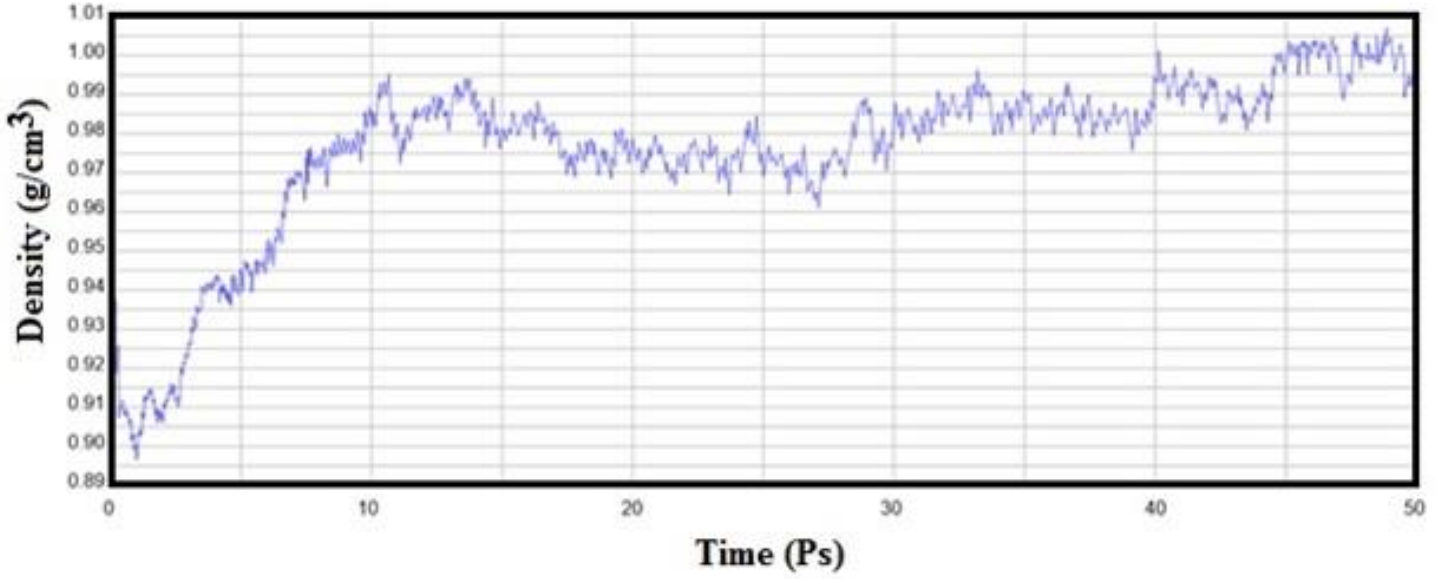


Fig. 5. Polyurethane polymer density diagrams in Materials Studio software

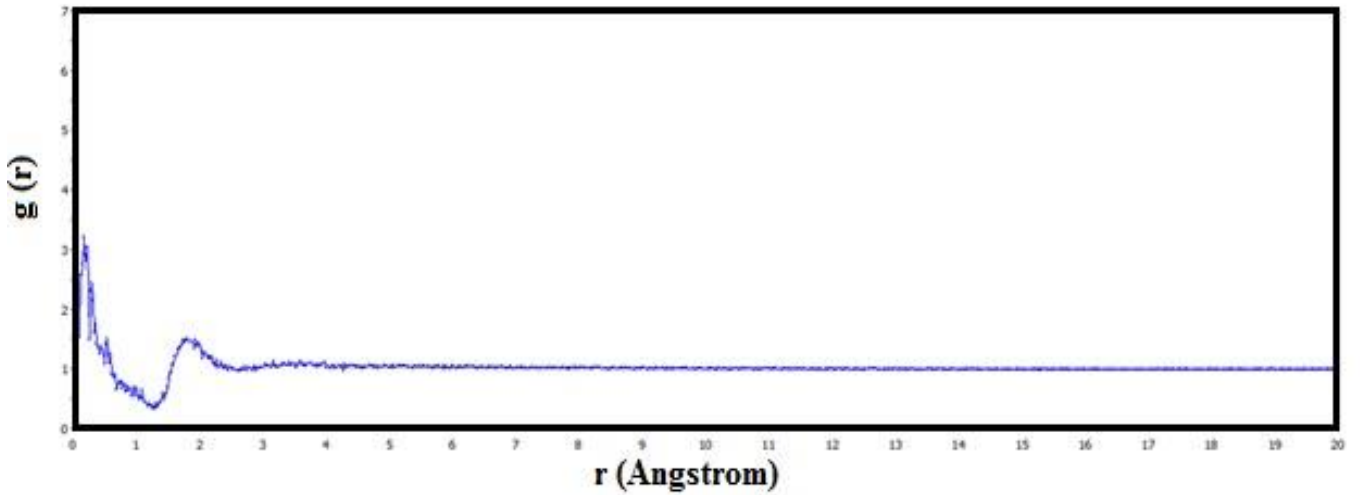


Fig. 6. Diagram of the RDF polyurethane polymer in the Materials Studio software

modate molecules and atoms at the best distance.

Fig. 4 applies NVT at 300 K in materials Studio software. One of the critical quantities to investigate the equilibrium validation of the system in molecular dynamics is the radial distribution function. The radial distribution function expresses the mass distribution of the system over atomic distances and is expressed Eq. (1).

$$g(r) = \frac{\rho(r)}{\rho} = \frac{\left[ N \left( r \pm \frac{\Delta r}{2} \right) \right]}{\Omega \left( r \pm \frac{\Delta r}{2} \right)} \frac{1}{\rho} \quad (1)$$

In this respect  $\frac{\rho(r)}{\rho}$  is the density of the number of atoms

in the shell to the radius  $r$  in volume  $\Omega \left( r \pm \frac{\Delta r}{2} \right)$  and  $\rho$  is

the density of the number of atoms in the total volume of the system. For solid materials, the radial distribution function at intervals the circle must converge to a numerical value, as shown in Fig. 5, and is a measure of the equilibrium of the solid atom's system. Two points are essential in this diagram: first, the convergence of the diagram to the number 1, indicating the correct execution of the distribution of atoms in the crystal structure. Second, the presence of sharp peaks in the graph indicates the formation of a solid structure by MDs, which demonstrates the accuracy of the modeling. Table 1 shows the mechanical and physical properties of the laboratory and analytical tests, which are very close,

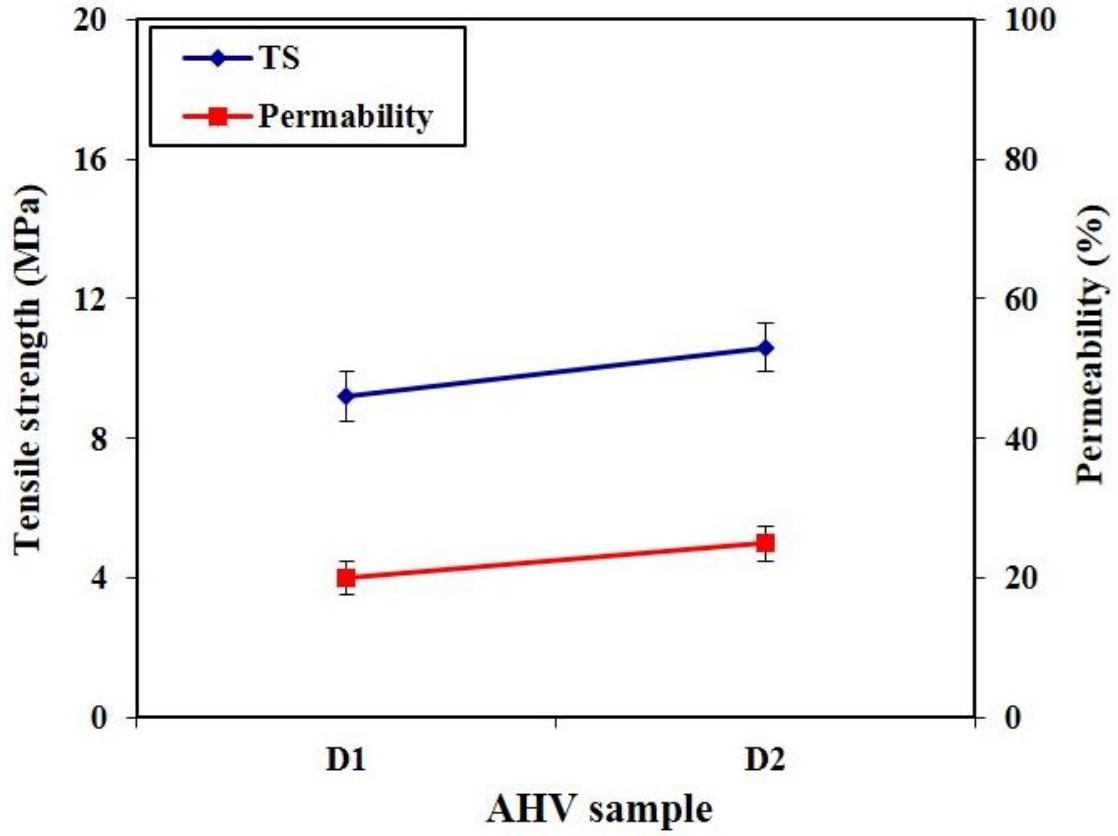


Fig. 7. Tensile strength and permeability value of AHV samples

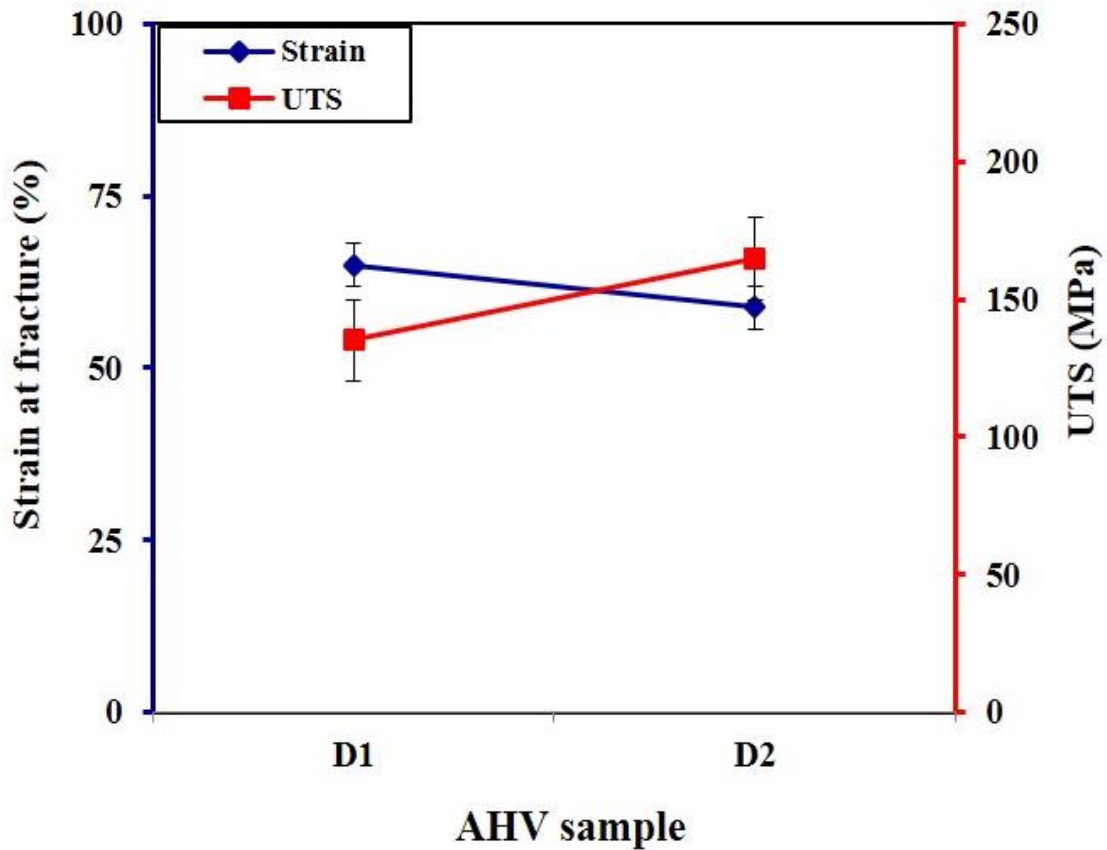


Fig. 8. Strain at fracture versus ultimate tensile strength value of AHV samples

while Fig. 6 describes the diagram of the radial distribution function (RDF) polyurethane polymer in the Materials Studio software. The following changes represent the relationship between the heart valve geometry and its tensile strength. Also, about 11% increase in diameter, lead to a nearly 0.09 increase in mechanical performance. Although as surface analysis indicated, the permeability of the inner and outer layer of the AHV is in the range of 20 and 25%. The diagram shows that tensile strength and permeability are both related to each other. Fig. 7 shows that the tensile strength of the AHV is in the range of 9.2 MPa to 10.6 MPa as the heart valve diameter changes from 14 mm to 16 mm. The strain at fracture value for the AHV decreases when increasing the diameter, while the ultimate tensile strength increased monotonously. The observation declares that strain at fracture point is not dependent on the ultimate tensile strength (UTS) value, as shown in Fig. 8. Previous researchers used ECM-coated molds in which living cells were extracted from the heart and replicated. These valves supported matrix and tissue regeneration. It has been shown that a fully synthetic heart valve (metallic or polymeric), which was made of animal protein tissue, can be applied as a human heart valve. Studies also showed that new generations of AHV in which currently available have a spring-like microstructure around the valve and tissue. This spring can be fully attached to the surroundings of the heart valve.

#### 4. CONCLUSIONS

A new AHVs was manufactured in the desired shape and size in only several minutes. So, this research aimed to develop a method for producing an AHV in minimum time and at a low cost. The data derived from the experimental test was then used to obtain mechanical properties (Young's modulus and Poisson's Ratio), physical properties (density) by using MDs, and also using the universal force field to predict mechanical and physical properties. It should be noted that this polymer was constructed with 2700 carbon atoms, 3600 hydrogen atoms, 200 nitrogen atoms, and 1000 oxygen atoms, and its structure is cubic in shape and lattice dimensions are  $35 \times 35 \times 35$  angstroms ( $\text{Å}^\circ$ ).

#### REFERENCES

- [1] J.N. Saour, J.O. Sieck, L.A.R. Mamo, A.S. Gallus, Trial of different intensities of anticoagulation in patients with prosthetic heart valves, *N. Engl. J. Med.* 322 (1990) 428–432.
- [2] W. Vongpatanasin, L.D. Hillis, R.A. Lange, Prosthetic heart valves, *N. Engl. J. Med.* 335 (1996) 407–416.
- [3] K.K. Yeo, N.D.M. Foin, Device for cardiac valve repair and method of implanting the same, (2019).
- [4] J.W. Eikelboom, S.J. Connolly, M. Brueckmann, C.B. Granger, A.P. Kappetein, M.J. Mack, J. Blatchford, K. Devenny, J. Friedman, K. Guiver, Dabigatran versus warfarin in patients with mechanical heart valves, *N Engl J Med.* 369 (2013) 1206–1214.
- [5] J. Yang, M.L. Pease, S.H. Heneveld, B.G. Walsh, Methods and apparatuses for deploying minimally-invasive heart valves, (2016).
- [6] P. Pibarot, J.G. Dumesnil, Prosthetic heart valves: selection of the optimal prosthesis and long-term management, *Circulation.* 119 (2009) 1034–1048.
- [7] E. Karamian, A. Nasehi, S. Saber-Samandari, A. Khandan, Fabrication of hydroxyapatite-baghdadite nanocomposite scaffolds coated by PCL/Bioglass with polyurethane polymeric sponge technique, *Nanomedicine J. 4* (2017) 177–183.
- [8] M. Razavi, A. Khandan, Safety, regulatory issues, long-term biotoxicity, and the processing environment, in: *Nanobiomaterials Sci. Dev. Eval.*, Elsevier, 2017: pp. 261–279.
- [9] A. Khandan, H. Jazayeri, M.D. Fahmy, M. Razavi, Hydrogels: Types, structure, properties, and applications, *Biomater Tissue Eng.* 4 (2017) 143–169.
- [10] S.J. Rowe, L. Wood, H. Bourang, G. Bakis, B. Spenser, N. Benichou, Y. Keidar, A. Bash, Methods for rapid deployment of prosthetic heart valves, (2010).
- [11] M.A. Salami, F. Kaveian, M. Rafienia, S. Saber-Samandari, A. Khandan, M. Naeimi, Electrospun polycaprolactone/lignin-based nanocomposite as a novel tissue scaffold for biomedical applications, *J. Med. Signals Sens.* 7 (2017) 228.
- [12] A. Farazin, H.A. Aghdam, M. Motififard, F. Aghadavoudi, A. Kordjamshidi, S. Saber-Samandari, S. Esmaeili, A. Khandan, A polycaprolactone bio-nanocomposite bone substitute fabricated for femoral fracture approaches: Molecular dynamic and micro-mechanical Investigation, *J. Nanoanalysis.* (2019).
- [13] B. Kamyab Moghadas, M. Azadi, Fabrication of Nanocomposite Foam by Supercritical CO<sub>2</sub> Technique for Application in Tissue Engineering, *J. Tissues Mater.* 2 (2019) 23–32.
- [14] B.K. Moghadas, A. Akbarzadeh, M. Azadi, A. Aghili, A.S. Rad, S. Hallajian, The morphological properties and biocompatibility studies of synthesized nanocomposite foam from modified polyethersulfone/graphene oxide using supercritical CO<sub>2</sub>, *J. Macromol. Sci. Part A.* 57 (2020) 451–460.
- [15] A. Kordjamshidi, S. Saber-Samandari, M.G. Nejad, A. Khandan, Preparation of novel porous calcium silicate scaffold loaded by celecoxib drug using freeze drying technique: Fabrication, characterization and simulation, *Ceram. Int.* 45 (2019) 14126–14135.
- [16] L.A. Harker, S.J. Slichter, Studies of platelet and fibrinogen kinetics in patients with prosthetic heart valves, *N. Engl. J. Med.* 283 (1970) 1302–1305.
- [17] H.M. Connolly, J.L. Crary, M.D. McGoon, D.D. Hensrud, B.S. Edwards, W.D. Edwards, H. V Schaff, Valvular heart disease associated with fenfluramine-phentermine, *N. Engl. J. Med.* 337 (1997) 581–588.
- [18] B. Lung, G. Baron, E.G. Butchart, F. Delahaye, C. Gohlke-Bärwolf, O.W. Levang, P. Tornos, J.-L. Vanoverschelde, F. Vermeer, E. Boersma, A prospective survey of patients with valvular heart disease in Europe: The Euro Heart Survey on Valvular Heart Disease, *Eur. Heart J.* 24 (2003) 1231–1243.
- [19] B.L. Roth, Drugs and valvular heart disease, *N Engl J Med.* 356 (2007) 6–9.
- [20] S.M. Mehta, T.X. Aufiero, W.E. Pae Jr, C.A. Miller, W.S. Pierce, Combined Registry for the Clinical Use of Mechanical Ventricular Assist Pumps and the Total Artificial Heart in conjunction with heart transplantation: sixth official report--1994., *J. Hear. Lung Transplant. Off. Publ. Int. Soc. Hear. Transplant.* 14 (1995) 585–593.
- [21] A. Bolz, M. Schaldach, Artificial heart valves: Improved blood compatibility by PECVD a-SiC: H coating, *Artif. Organs.* 14 (1990) 260–269.
- [22] L.P. Dasi, H.A. Simon, P. Sucusky, A.P. Yoganathan, Fluid mechanics of artificial heart valves, *Clin. Exp. Pharmacol. Physiol.* 36 (2009) 225–237.
- [23] X. Ye, Y. Shao, M. Zhou, J. Li, L. Cai, Research on micro-structure and hemo-compatibility of the artificial heart valve surface, *Appl. Surf. Sci.* 255 (2009) 6686–6690.
- [24] D.J. Evans, S. Murad, Singularity free algorithm for molecular dynamics simulation of rigid polyatomics, *Mol. Phys.* 34 (1977) 327–331.
- [25] S. Esmaeili, M. Shahali, A. Kordjamshidi, Z. Torkpoor, F. Namdari, S.S. Samandari, M. Ghadiri Nejad, A. Khandan, An artificial blood vessel

- fabricated by 3D printing for pharmaceutical application, *Nanomedicine J.* 6 (2019) 183–194.
- [26] C.G. Del, A. Bianco, M. Grigioni, Electrospun bioresorbable trileaflet heart valve prosthesis for tissue engineering: in vitro functional assessment of a pulmonary cardiac valve design., *Ann. Ist. Super. Sanita.* 44 (2008) 178–186.
- [27] S. Esmaeili, H.A. Aghdam, M. Motiffard, S. Saber-Samandari, A.H. Montazeran, M. Bigonah, E. Sheikhabahaei, A. Khandan, A porous polymeric-hydroxyapatite scaffold used for femur fractures treatment: fabrication, analysis, and simulation, *Eur. J. Orthop. Surg. Traumatol.* 30 (2020) 123–131.
- [28] M. Monshi, S. Esmaeili, A. Kolooshani, B.K. Moghadas, S. Saber-Samandari, A. Khandan, A novel three-dimensional printing of electroconductive scaffolds for bone cancer therapy application, *Nanomedicine J.* 7 (2020) 138–148.
- [29] M. Bahadori, M. Yaghoubi, E. Haghoshyie, M. Ghasemi, E. Hasanpoor, Patients' and physicians' perspectives and experiences on the quality of medical consultations: a qualitative evidence., *Int. J. Evid. Based. Healthc.* (2019).
- [30] M. Ghadirinejad, E. Atasoylu, G. Izbirak, M. GHA-SEMI, A Stochastic Model for the Ethanol Pharmacokinetics, *Iran. J. Public Health.* 45 (2016) 1170.
- [31] F. Aghadavoudi, H. Golestanian, Y. Tadi Beni, Investigating the effects of resin crosslinking ratio on mechanical properties of epoxy-based nanocomposites using molecular dynamics, *Polym. Compos.* 38 (2017) E433–E442. <https://doi.org/10.1002/pc.24014>.
- [32] farshid Aghadavoudi, H. Golestanian\*, Y. Tadi Beni, Investigation of CNT Defects on Mechanical Behavior of Cross linked Epoxy based Nanocomposites by Molecular Dynamics, *ADMT J.* 9 (2016).
- [33] R. Moradi-Dastjerdi, F. Aghadavoudi, Static analysis of functionally graded nanocomposite sandwich plates reinforced by defected CNT, *Compos. Struct.* 200 (2018) 839–848.
- [34] F. Aghadavoudi, H. Golestanian, K.A. Zarasvand, Elastic behaviour of hybrid cross-linked epoxy-based nanocomposite reinforced with GNP and CNT: experimental and multiscale modelling, *Polym. Bull.* 76 (2019) 4275–4294. <https://doi.org/10.1007/s00289-018-2602-9>.
- [35] M.A. Maghsoudlou, R.B. Isfahani, S. Saber-Samandari, M. Sadighi, Effect of interphase, curvature and agglomeration of SWCNTs on mechanical properties of polymer-based nanocomposites: Experimental and numerical investigations, *Compos. Part B Eng.* 175 (2019) 107119.
- [36] M. Motiffard, M. Pesteh, M.R. Etemadifar, S. Shirazinejad, Causes and rates of revision total knee arthroplasty: Local results from Isfahan, Iran, *Adv. Biomed. Res.* 4 (2015).
- [37] S. Sahmani, A. Khandan, S. Esmaeili, S. Saber-Samandari, M.G. Nejad, M.M. Aghdam, Calcium phosphate-PLA scaffolds fabricated by fused deposition modeling technique for bone tissue applications: Fabrication, characterization and simulation, *Ceram. Int.* 46 (2020) 2447–2456.
- [38] M. Nourbakhsh, M. Motiffard, H. Shemshaki, M. reza Etemadifar, A. Zarezade, Z. Farajzadegan, F. Mazoochian, Efficacy of tibial proximal osteotomy in correction of lower limb alignment indexes in patients with osteoarthritis in medial compartment of knee, *Med. Arch.* 66 (2012) 58.
- [39] M.A. Tahririan, M. Motiffard, A. Omidian, H.A. Aghdam, A. Esmaeali, Relationship between bone mineral density and serum vitamin D with low energy hip and distal radius fractures: A case-control study, *Arch. Bone Jt. Surg.* 5 (2017) 22.
- [40] M. Motiffard, M. Heidari, A. Nemati, No difference between wound closure in extension or flexion for range of motion following total knee arthroplasty: a randomized clinical trial, *Knee Surgery, Sport. Traumatol. Arthrosc.* 24 (2016) 74–78.
- [41] H.A. Aghdam, E. Sanatizadeh, M. Motiffard, F. Aghadavoudi, S. Saber-Samandari, S. Esmaeili, E. Sheikhabahaei, M. Safari, A. Khandan, Effect of calcium silicate nanoparticle on surface feature of calcium phosphates hybrid bio-nanocomposite using for bone substitute application, *Powder Technol.* 361 (2020) 917–929.
- [42] R. Moradi-Dastjerdi, G. Payganeh, M. Tajdari, Resonance in functionally graded nanocomposite cylinders reinforced by wavy carbon nanotube, *Polym. Compos.* 38 (2017) E542–E552.
- [43] M. Moeini, R. Barbaz Isfahani, S. Saber-Samandari, M.M. Aghdam, Molecular dynamics simulations of the effect of temperature and strain rate on mechanical properties of graphene-epoxy nanocomposites, *Mol. Simul.* 46 (2020) 476–486.
- [44] M. Hadipeykani, D. Toghraie, Thermomechanical Properties of the Polymeric Nanocomposite Predicted by Molecular Dynamics, *ADMT J.* 12 (2019) 25–32.
- [45] A. Farazin, F. Aghadavoudi, M. Motiffard, S. Saber-Samandari, A. Khandan, Nanostructure, molecular dynamics simulation and mechanical performance of PCL membranes reinforced with antibacterial nanoparticles, *J. Appl. Comput. Mech.* (2020).

#### HOW TO CITE THIS ARTICLE

Z. S. Kazerouni, M. Telloo, A. Farazin, S. Saber-Samandari, E. Sheikhabahaei, B. Kamyab-Moghadas, H. Joneidi -Yekta, S. Esmaeili, A. Khandan, A Mitral Heart Valve Prototype Using Sustainable Polyurethane Polymer: Fabricated by 3D Bioprinter, Tested by Molecular Dynamics Simulation, *AUT J. Mech. Eng.*, 5(1) (2021) 109-120.

DOI: [10.22060/ajme.2020.17450.5862](https://doi.org/10.22060/ajme.2020.17450.5862)



